



# Influencing the Wettability of HSS-Steels by Addition of Alloying Elements to the Zinc Bath

Guizhi Zeng, Bernd Friedrich

IME Process metallurgy and metal recycling department and chair of RWTH Aachen University,  
Intzestraße 3,  
52056 Aachen, Germany

---

## Abstract

The containing of high amounts of alloying elements such as Si, P, Mn reduces dramatically the wettability of High Strength Steels (HSS) and therefore, deteriorates their coating quality from continuous hot-dip-galvanizing in conventional Al alloyed Zinc baths. In this paper, the wetting behavior of different Zn alloys (Ca, Mg, Cu, Ni, Ti, V, Zr, Y, Ce, La) on three special types of steel substrates have been investigated. Firstly, the surface tensions of these Zinc alloys were calculated based on thermochemical databases and modelling. Then the wetting angels of these Zn alloys on the steel substrates are measured via the sessile drop method. By comparing the final shape of their droplets formed on the steel substrates, a qualitative series of the influence of the alloying elements was obtained. The wettability of the same zinc alloy with the high alloyed DP500 steel is worse than with normal M3A13 steel and low alloy 31AXV steel. Under a reductive hydrogen atmosphere, their wetting behavior can be strongly increased in compare to that of under a 95% argon-5% hydrogen atmosphere. Among the investigated Zn containing alloys, Vanadium and Zirconium as alloying elements show the most effective improvement of the wettability on high strength steel substrates.

## Keywords:

Wettability, Wetting Angle, Zinc Alloy, High Strength Steel, Hot-dip Galvanizing.



# 1 Introduction

The growing demands of weight reduction and passenger safety in automobile, promote the application of high strength steels (HSS) sheets in the construction of the car bodies steadily. The ULSAB-AVC program (Ultra Light Steel Auto Body - Advanced Vehicle Concept [1]) expects that 80% of steels used in automobile industry should be either DP (dual phase) or TRIP (transformation induced plasticity) steels. Comparing to conventional unalloyed and low alloyed steels, HSS are nowadays usually alloyed with a high amounts of Si, Mn, Cr together with other elements, in order to achieve both higher tensile strength and better formability [1].

In order to protect the steel sheets against corrosion, a layer of zinc or zinc alloy is always coated on the surface of the steel sheets, mostly achieved by hot dip galvanizing (HDG) the strip prior to pressing. However, the increased amounts of alloying elements like P, Mn or Si in the high strength steels causes problems in the zinc galvanizing process. Prior to immersion into the HDG bath, the Fe-oxide and Fe-hydroxide layer created during the cold rolling process is completely removed in an annealing furnace. During this treatment the main alloying elements of HSS (e.g. Mn, Si, Al, Cr, V and Ti), which have strong affinity towards oxygen, will migrate preferentially through easy diffusion paths, such as grain and sub grain boundaries, to the substrate surface and are oxidized there [2]. The oxidation products do not form a continuous layer on the surface but are present as dispersed islands, which will strongly deteriorate the wettability of the steel strip surface and result in a poor coating quality. Elements like Si and P will also influence the kinetics and velocity of the reactions between zinc and iron during the galvanizing process [3]. Depending on the Si and P content a strong irregular layer grows with an inhomogeneous surface construction, which again will damage the adhesion and wetting behavior between Zn melt and steel strips.

To reduce the deterioration of the alloying elements and improve the adhesion of the zinc coating, on one hand the steel substrate should be pre-treated to change the chemical composition and to prevent the external oxidation of the alloying elements at the surface. This can be achieved by annealing in reactive atmosphere, where reducing, nitriding or carburizing occurs [4]. On the other hand, reactive alloying elements could be added into the zinc bath, in order to increase the reactivity between zinc and the steel surface, such improving the wettability and the adhesion of the zinc coating.

Aluminium is one of the most effective alloying elements to reduce the influence of Si in steel during Zinc galvanizing. Aluminium in the range of 0.1-0.3 wt% is added to the continuous zinc galvanizing bath to suppress the growth of brittle Fe-Zn intermetallic phases at the steel coating interface by forming of a  $\text{Fe}_2\text{Al}_5$  inhibition layer [6]. Zn-Al baths with a reactive third alloy element were commercially produced for strip HDG, such as Galfan (95% Zn, 5% Al, traces of “Mischmetal” containing Cerium and Lanthanum), Lavagal (35% Al-Zn-Na-Mg) and Galvalume (55% Al, 43.3% Zn, 1.6% Si). The addition of Mischmetal improves the wettability and fluidity of the molten zinc bath and such avoid the formation of the brittle intermetallic phase between the steel substrate

and the coating. This finally leads to a significant increase in formability and corrosion life of the steel strip [7].

It is also reported that the presence of Ni (0.08 - 0.1%) in Zinc HDG baths, known as Technigalva, reduces substantially the thickness and corrosion rate of the galvanized coating by suppressing the reactivity of steel containing up to 0.25% Si [7]. Katiforis and Papadimitriou have studied the influence of copper, cadmium and tin on the constitution and the thickness of the coatings [5]. They have shown that copper forms a ternary Fe-Zn-Cu intermetallic compound, promotes the  $\delta$ 1 phase formation, hinders the  $\zeta$  phase growth and results in a worse adherence of the coating. Cadmium with a concentration above 1 wt.-% promotes the  $\zeta$  phase and  $\Gamma$  phase and hinders the growth of the  $\delta$ 1 phase. By addition of up to 3 wt.-% tin no significant changes in morphology and thickness of the obtained galvanized coatings occur. Reumont et. al. have reported that the Sandelin-effect can be prevented if  $>0.025\%$  Ti was contained in the zinc bath [8].

This paper presents the results of a German DFG research project, where various elements (Ca, Mg, Cu, Ni, Ti, V, Zr, Y, Ce, La), which have a particular big affinity to oxygen, were alloyed with Zn to investigate their influences on the wetting behavior and reaction kinetic between Zinc and special steels. The surface tension of these zinc alloys was firstly calculated on the basis of thermochemical data of its pure elements. Their wetting behaviors on different steel sheets (normal M3A13 steel, low alloyed 31AXV steel and high alloyed DP500 steel) have been studied by means of the sessile drop method. SEM and WDX methods were used to analyze the microstructure and component distribution of the coating layers.

## 2 Thermochemical evaluation of surface properties

### 2.1 Wetting angle and surface tension

The wettability of a liquid is quantified by the wetting angle between the interface of the liquid phase and surface of the solid phase, when a liquid droplet is in thermal equilibrium with a horizontal solid surface, as shown in Figure1. Generally, when the wetting angle  $\theta$  ranges between  $0^\circ$  and  $90^\circ$ , the surface is strongly or partially wetting. The liquid does not wet the surface significantly if the wetting angle  $\theta$  ranges between  $90^\circ$  and  $180^\circ$ . If the wetting angle is equal to  $0$ , the liquid is perfect wetting and it spreads spontaneously over the solid surface, the ideal situation for a HDG process. For wetting angle equaling to  $180^\circ$ , the liquid is called perfectly non-wetting.

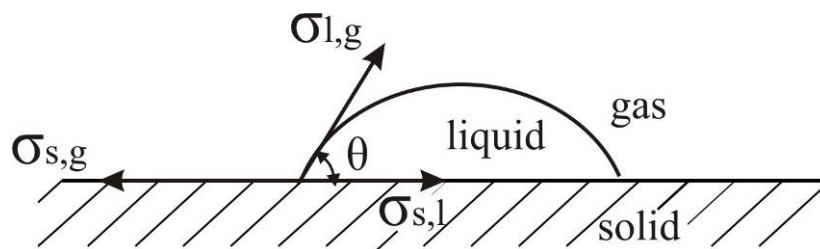




Figure 1: Contact angle and balance of interfacial forces

The value of wetting angle  $\theta$  is determined at the force equilibrium built up by the interfacial tensions of solid-gas  $\sigma_{s,g}$ , liquid-gas  $\sigma_{l,g}$  and solid-liquid  $\sigma_{s,l}$  in relation of the Young's equation [9]:

$$\sigma_{l,g} \cos \theta = \sigma_{s,g} - \sigma_{s,l} \quad (1)$$

Girifalco and Good have derived the following expression for the interfacial tension  $\sigma_{s,l}$  between the liquid and solid phase [10]:

$$\sigma_{s,l} = \sigma_{s,g} + \sigma_{l,g} - 2\Phi \sqrt{\sigma_{s,g} \sigma_{l,g}} \quad (2)$$

where  $\Phi$  is the interaction parameter, which depends on the type of atomic/molecular bonding between the liquid and solid phases. Combining equations (1) and (2), the wetting angle  $\theta$  can be expressed by:

$$\cos \theta = 2\Phi \sqrt{\frac{\sigma_{s,g}}{\sigma_{l,g}}} - 1 \quad (3)$$

According to equation (3), it can be seen that if the surface tension of the liquid  $\sigma_{l,g}$  is kept as small as possible, the value of  $\cos \theta$  increases, which means that the wetting angle  $\theta$  decreases and so that the wettability between the liquid droplet and solid surface increases.

## 2.2 Theory for thermochemical modelling of surface tension

According to Gibbs' adsorption theory, the surface phase and the bulk phase of alloys are considered to be in thermochemical equilibrium, the chemical potential of each alloy component  $i$  in the monolayer surface is equal to that of the corresponding component in the bulk phase. Therefore, the surface tension  $\sigma$  of alloy can be expressed as:

$$\sigma = \frac{\mu_i^{oS} - \mu_i^{oB}}{\bar{S}_i} + \frac{RT}{\bar{S}_i} \ln \frac{a_i^S}{a_i^B} \quad (4)$$

( $\sigma$  is the surface tension,  $\mu_i^{oS}$ ,  $\mu_i^{oB}$  are the standard chemical potential of component  $i$  in the surface phase and the bulk phase,  $a_i^S$ ,  $a_i^B$  are the activity of the component  $i$  in the surface phase and bulk phase,  $R$  is the universal gas constant,  $T$  is the absolute temperature,  $\bar{S}_i$  is the partial molar surface area of component  $i$ )

Assuming that no volume effects in the surface occur by mixing, so that the partial molar surface area of one of component  $i$   $\bar{S}_i$  is equal to the molar surface area  $S_i$  of pure component  $i$ , it is possible to derive the Butler's equation relative to one of the components [11]:



$$\sigma = \sigma_i^o + \frac{RT}{S_i} \ln \frac{a_i^S}{a_i^B} = \sigma_i^o + \frac{RT}{S_i} \ln \frac{X_i^S}{X_i^B} + \frac{RT}{S_i} \ln \frac{\gamma_i^S}{\gamma_i^B} \quad (5)$$

with  $\sigma_i^o = (\mu_i^{oS} - \mu_i^{oB})/S_i$  as the surface tension of the pure component  $i$ ;  $X_i^S$  and  $X_i^B$  denote the mole fractions and  $\gamma_i^S$  and  $\gamma_i^B$  are the activity coefficients of the component  $i$  in surface phase and in the bulk phase. Such the surface tension of a binary alloy system can be expressed based on the surface tension of their pure elements as follows:

$$\sigma = \sigma_1^o + \frac{RT}{S_1} \ln \frac{X_1^S}{X_1^B} + \frac{RT}{S_1} \ln \frac{\gamma_1^S}{\gamma_1^B} = \sigma_2^o + \frac{RT}{S_2} \ln \frac{X_2^S}{X_2^B} + \frac{RT}{S_2} \ln \frac{\gamma_2^S}{\gamma_2^B} \quad (6)$$

In assumption of a perfect surface solution model with ideal behavior of the bulk and surface phases, the activity coefficients of the component  $i$  in surface phase equals to that of in the bulk phase:  $\gamma_i^S = \gamma_i^B$ . On the basis of  $X_1^S + X_2^S = 1$ , the following equation can be obtained: [11]

$$X_1 \exp\{(\sigma - \sigma_1^o)S_1/RT\} + X_2 \exp\{(\sigma - \sigma_2^o)S_2/RT\} = 1 \quad (7)$$

By using the expansion  $\exp \varphi = 1 + \varphi$ , the surface tension of the binary alloy can be calculated relative to the surface tension of pure component 1 and 2:

$$\sigma = \frac{X_1 \sigma_1^o S_1 + X_2 \sigma_2^o S_2}{X_1 S_1 + X_2 S_2} \quad (8)$$

For ternary alloys, the calculation of surface tension can be derived in the similar way as in the binary systems:

$$\sigma = \frac{X_1 \sigma_1^o S_1 + X_2 \sigma_2^o S_2 + X_3 \sigma_3^o S_3}{X_1 S_1 + X_2 S_2 + X_3 S_3} \quad (9)$$

The surface areas  $S_i$  of the pure elements at the relevant temperatures can be calculated from the densities of corresponded elements by the Brandes' equation [11]:

$$S_i = kN^{1/3}V_i^{2/3}$$

where  $k$  is a geometric factor with a value of 1.091 for a closed packed lattice,  $N$  is the Avogadro's number with a value of  $6.02 \times 10^{23}$  and  $V_i$  is the molar volume of the component  $i$  determined from its density.

It was found that the molar volume  $V_i$  and surface tension  $\sigma_i$  of pure elements in alloys are linearly depending on the temperature, based on their values  $V_{m,i}$  and  $\sigma_{m,i}$  at the melting temperature,  $T_{m,i}$ : [12]



$$V_i = V_{m,i} \{1 + \alpha_i (T - T_{m,i})\} \quad (11)$$

$$\sigma_i = \sigma_{m,i} + \frac{d\sigma_i}{dT} (T - T_{m,i}) \quad (12)$$

## 2.3 Surface tension calculation of zinc alloys

According to the described theory, the surface tension  $\sigma$  of binary zinc alloys ZnX and ternary ZnAl0.2X was calculated at the assumption of a perfect surface solution model by combining the equations (8) to (12). The molar volume  $V_i$  and surface tension  $\sigma_i$  of pure alloying elements in zinc alloys at different temperature were calculated by using standard thermochemical data, leading to the values shown in Table 1.

Table 1: Molar volume and surface tensions of pure elements [12]

Element	$T_{m,i}$ (K)	$V_i = V_{m,i} \{1 + \alpha_i (T - T_{m,i})\}$		$\sigma_i = \sigma_{m,i} + \frac{d\sigma_i}{dT} (T - T_{m,i})$	
		$V_{m,i}$ ( $10^{-6} \text{m}^3 \cdot \text{mol}^{-1}$ )	$\alpha_i$ ( $10^{-4} \text{K}^{-1}$ )	$\sigma_{m,i}$ ( $\text{mN} \cdot \text{m}^{-1}$ )	$d\sigma_i/dT$ ( $\text{mN} \cdot \text{m}^{-1} \cdot \text{K}^{-1}$ )
Zn	692.62	9.94	1.5	782	-0.17
Al	933.35	11.3	1.5	914	-0.35
Ca	1124.15	29.5	1.6	361	-0.10
Mg	923.15	15.3	1.6	559	-0.35
La	1193.15	23.3	0.4	720	-0.32
Ce	1068.15	20.9	0.34	740	-0.33
Y *	1796.15	21.42	0.51	804	-0.05
Cu	1356.15	7.94	1.0	1303	-0.23
Zr	2130.15	15.4	0.54	1480	-0.20
Ti	1998.15	11.6	0.56	1650	-0.26
Ni	1728.15	7.43	1.51	1778	-0.38
V	1973.15	9.5	0.6	1950	-0.31

Note: \* reference from [13].

Figure 2 left shows the calculated surface tensions of ZnX binary alloys with a molar fraction of X from 0 to 0.2% and Figure 2 right those of ZnAl0.2X ternary alloys which contain 0.2% of Al having the same molar fraction of X. The temperature used for calculation is set to 500°C, which is a typical temperature for zinc galvanizing. Comparing Figure 2, it can be seen that in both alloy systems each element X shows similar influences to the total surface tension. With the addition of Ca and Mg, which has a low surface tension at its melting temperature  $\sigma_{m,i}$ , the surface tension of their



Zn alloys decreases as well as the composition of the alloying element increases. There are no big variations in the surface tension of Zn alloys containing Ce, La and Y. By adding Cu, Zr, Ti, Ni and V the surface tension of the ZnX and ZnAl0.2X increased.

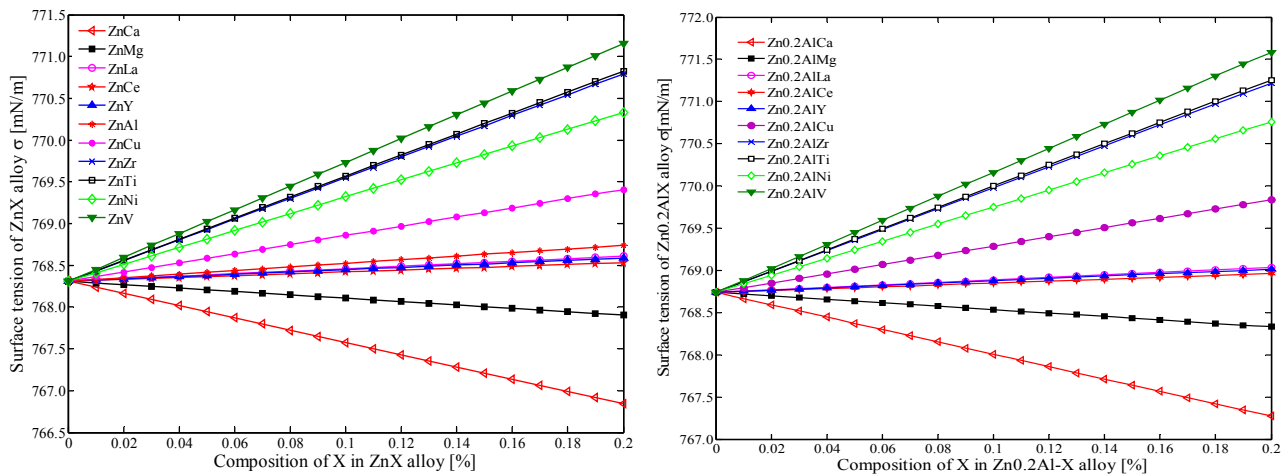
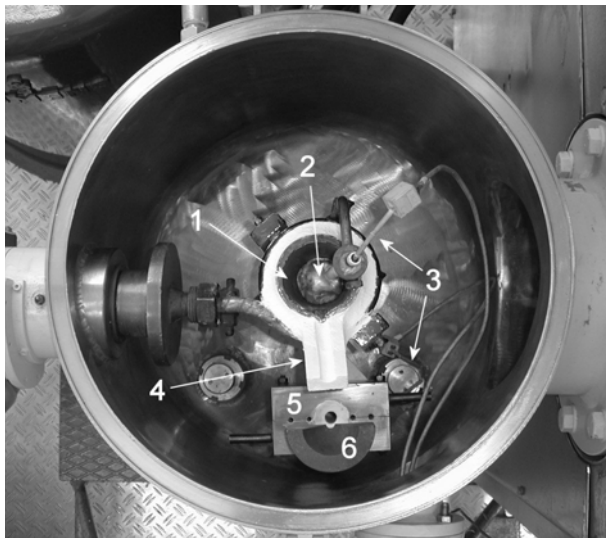


Figure 2: The surface tension of binary ZnX alloys (left) and ternary ZnAl0.2X alloys (right) with composition of X from 0 to 0.2% at a temperature of 500°C

### 3 Experimental

Different alloying elements Ca, Ce, Cu, La, Mg, Ni, Ti, V, Y and Zr, were chosen to form alloys with Zinc for an experimental wettability study. These elements have relative big affinity to oxygen in order to reduce the formation of the troublesome metal oxide ( $\text{SiO}_2$ ,  $\text{MnO}$ ,  $\text{P}_2\text{O}_5$ ), which disturb the good adhesion between Zn on steel.

The melting temperatures of all these alloying elements are considerably higher than the melting point of the basis metal zinc (419.58°C), some of them are over 1000°C, as shown in Table 1. In order to avoid massive evaporation of zinc, the maximum alloying temperature were set below 700°C. Among these alloying elements, only Cu and Mg are completely soluble in zinc with alloy composition of ZnX0.05, ZnX0.2 and ZnAl0.2X0.2. Most of them are not soluble in solid zinc but build intermetallic phases with zinc. These alloy elements were at first pre-alloyed with pure zinc (> 99.995 % Zn) to obtain relative higher alloy composition or as high as possible. Then the pre-alloy is melted with a respectively calculated mass of pure zinc to manufacture the final alloys with accurate alloy compositions. Both the pre-alloy and the final alloy process were conducted under Argon atmosphere in a sealed induction furnace. The casting mould was placed near the crucible inside the sealed furnace, which is shown in Figure 3, so that the melted alloy can be casted under inert atmosphere as well.



1. ceramic crucible
2. smelter
3. thermocouple
4. pouring spout
5. casting mould
6. casting funnel

Figure 3: The work room of the induction furnace.

A self designed casting mould, as shown at the left side in Figure 4, was used for casting. The melting zinc alloys was poured through the centre column of the mould and then the liquid flows to the bottom of the mould separately at both side. As the bottom column was filled up, the excess liquids flow from bottom upon at the rest four parallel columns with rod length of 12 mm and diameter of 5mm at the same time. The flow direction and the obtained rod ingot are shown at the right side of Figure 4. By using this bottom casting technology, the impurities and slag rest formed in the smelting can be excluded in the centre column and alloy with more accurate composition and more homogeneous composition distribution can be gained from the four side columns. The manufactured zinc alloy ingot was then cut into small cylinders with a length of 3 mm for further wettability tests.

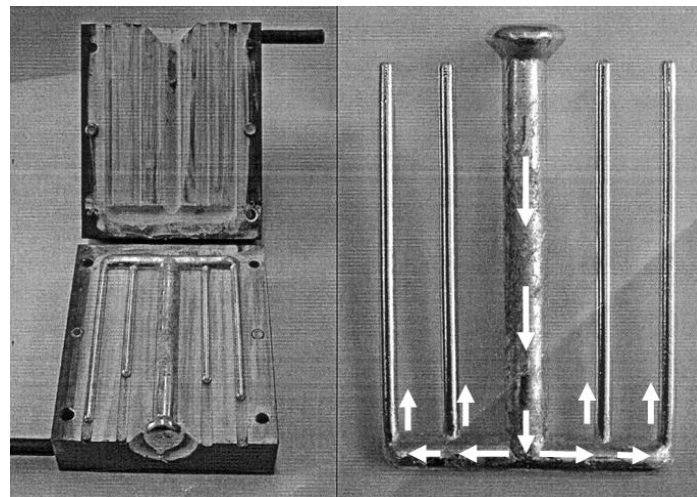


Figure 4: The opened casting mould (left) and the casted ingot (right)

The wetting angles of these zinc alloy droplets on the flat steel substrates were measured by means of the sessile drop method. The schematic illustration of the whole setup for the measurement of wetting angle is shown in Figure 5. The experiments were conducted in a self designed electrical





resistance furnace with a tightly sealed quartz glass tube (Figure 6). The temperature inside the furnace was controlled by a PID electrical heater. The picture of the formed droplet was taken by a CCD camera OCA and the wetting angle between droplet of Zn alloy and the steel substrate can be measured by the equipment SCA20 from Dataphysics Instrument GmbH. The wettabilities of Zn alloy to three special types of steel substrates (high strength steel DP500, low alloyed steel 31AXV and normal steel M3A13) with chemical compositions shown in Table 2 were compared.

Table 2: Chemical composition of tested steels in wt.-%

	C	Si	Mn	P	S	Cr	Mo	Ni	Al	Ti
DP500	0.064	0.13	1.46	0.013	0.003	0.34	0.19	0.03	0.034	<0.001
31AXV	0.006	0.004	0.19	0.012	0.007	0.017	-	0.017	0.016	0.0007
M3A13	0.002	0.067	0.26	0.011	0.003	0.019	-	0.018	0.031	0.018

Before each experiment, the steel substrate samples were mechanically polished by emery paper and then degreased with alcohol and pickled in a 10% diluted HCl for about 10 seconds at 60 °C to remove the oil and oxide film from the steel surfaces. The cleaned steel substrate were then rinsed with distilled water and immersed into an ascorbic acid bath for around 5 seconds to minimize further oxidation of the steel surface and then placed above a graphite table with inclined hole for thermocouple to measure the real temperature of the steel substrate.

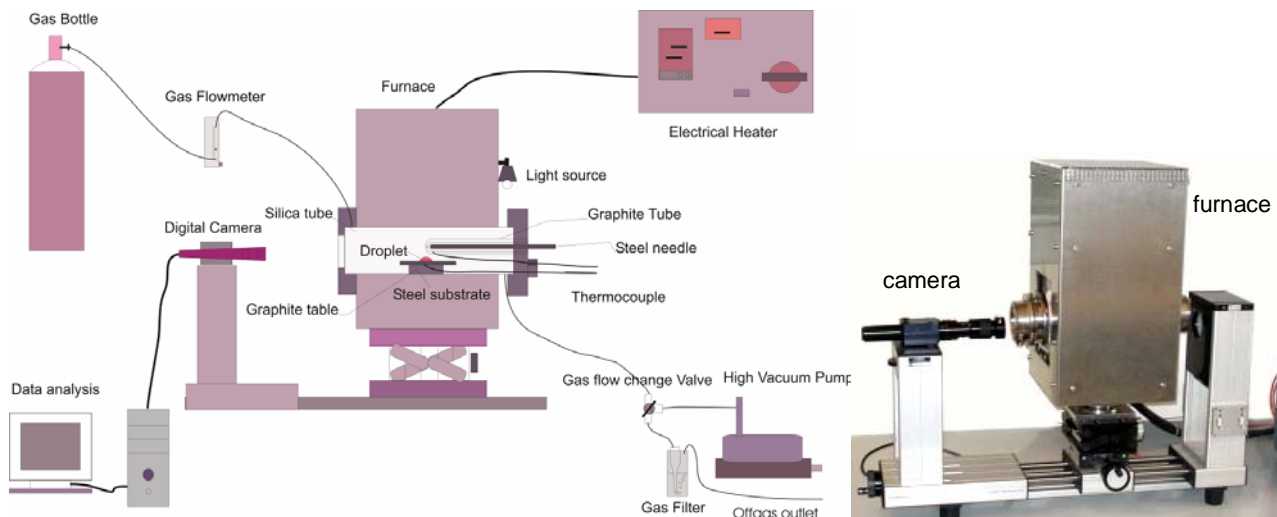


Figure 5: Illustration of the whole experimental setup

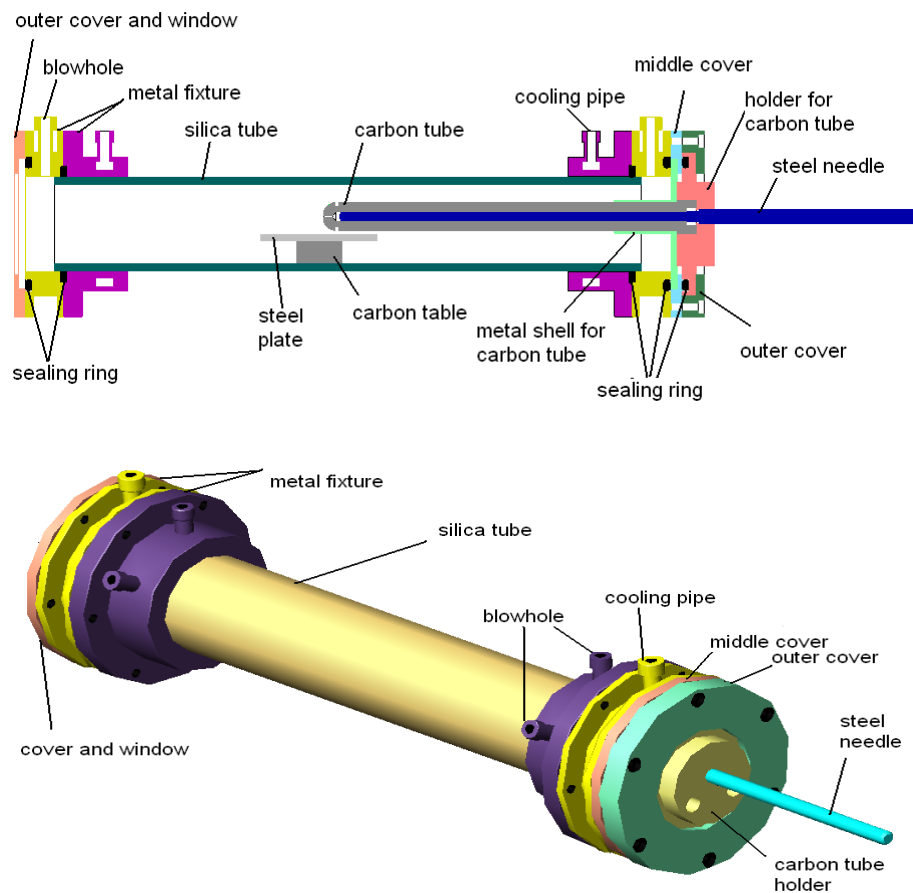


Figure 6: Detailed schematic of the set up of droplet forming system

The Zinc alloy samples were filled at the front end of a graphite tube fixed by a metal holder on the silica tube as shown in Figure 6. A groove was designed at the front end of the graphite tube for held thermocouple to measure the real temperature of the zinc alloy samples. As the samples were prepared and the furnace was sealed, the sealed silica tube was firstly evacuated for 10 minutes by a mechanical vacuum pump and then backfilled with inert gas (pure hydrogen or pure hydrogen) with a flow rate of about 20ml/min. The electrical heater is turned on to heat up the zinc samples inside the furnace to the experimental temperature 500°C, where it was held for 30 minutes to allow the zinc alloy melting completely. Meanwhile, the metal holder was cooled by running water through the cooling pipe at the end of the silica tube to protect the gummy sealing ring, as shown in Figure 6. When the zinc alloy samples were completely smelt, the molten zinc alloy inside the graphite tube was pushed out by the stainless steel screw and an alloy droplet fell down onto the steel substrate placed below.

The shape change of the formed droplets with time can be recorded by a high speed digital camera OCA from Dataphysics Instrument GmbH through the glass window of the furnace. The wetting angle between and Zn alloy droplet and the steel substrates was then calculated by the graphical analysis program SCA20also from Dataphysics Instrument GmbH. The baseline and the outline of the droplet were defined automatically or manually when necessary. With the definition of both

lines an iterative process is initiated to get the three phase point, the cross point of the outline and the baseline. The contact angle of the droplet is the angle between the baseline and the tangents of the outline. The value of the contact angle is then read by the scale around as shown in Figure 8.

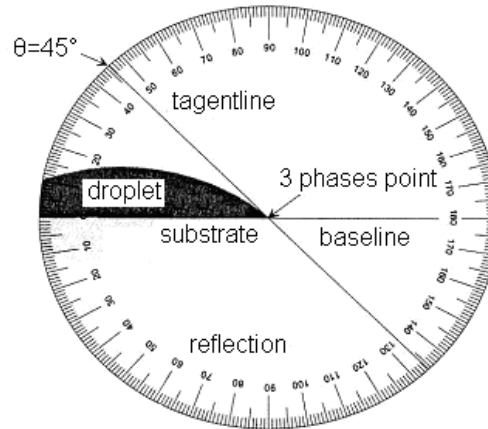


Figure 8: The principle of the contact angle measurement

After experiments, the surface appearances of the steel substrates samples adhered with zinc alloy droplets were recorded by normal digital camera initially. The cross sections of some samples are embedded in resin and then mechanical polished and carbon coated for scanning electron microscope (SEM) analysis of the morphology of the formed droplet by ZEISS DSM 962 SEM analysis machine. Oxford ISIS electron - dispersive spectroscopy EDS and wavelength - dispersive spectroscopy (WDS) were attached and used to chemically analyze the distribution and diffusion behaviors of Zn, Fe and other alloying elements.

## 4 Results and discussion

### 4.1 Dynamic change of the wetting angle

As the liquid droplet of zinc alloy is contacting with the steel substrate, the shape of the droplet decreases dramatically. It takes normally only a few seconds till it completely solidifies and reaches equilibrium. Figure 7 shows the shape changes of a ZnCe0.2 droplet from a half ball (non wetting) to a flattened lens (good wetting) within 4 seconds after contacting the steel surface. This dynamic change of the wetting angle between the liquid Zn alloy droplet and

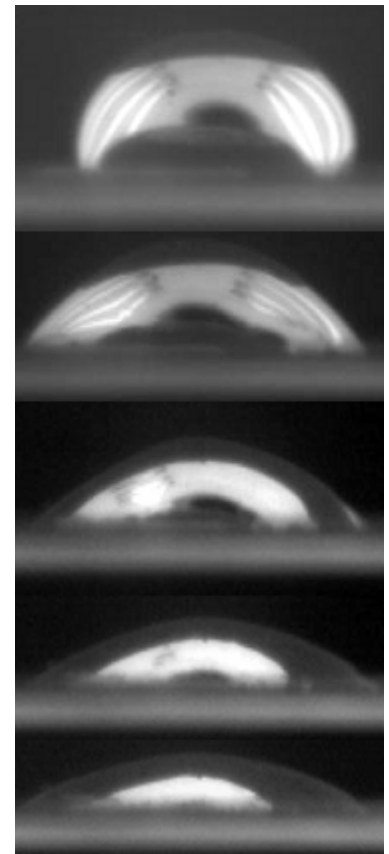


Figure 7: Dynamic variation of the shape of a ZnCe0.2 droplet after contacting a steel substrate

the steel substrate is influenced by multiple factors. The main factors are diffusion and reaction interactions between liquid zinc and its alloying elements and iron with its alloying elements. The Zn-alloy droplet begins to be solidified after the very first contact with the substrate. At the same time, zinc is evaporated from the surface of the droplet, whose effect can be also observed as a shadow in Figure 7. Furthermore, the alloying elements existed in Zn alloy with a relative high oxygen affinity react with the residual oxygen remained in the furnace atmosphere and affect the wetting behavior of the droplet as well. Finally, the gravity force of the droplet itself influences the force equilibrium and the final shape of the droplet. Therefore, it is necessary to keep the droplet in a comparable mass and to measure the contact angle after the same contact time, in order to compare the contact angle of the droplets of different Zn alloys.

## 4.2 The influence of alloying elements on wettability

First of all, the wettability was able to be qualitatively compared by the final shape of formed droplet after the solidification. Such, the final shape of the droplet after solidification was divided into four types: a sphere, a flattened sphere, a cap, and a lens, which are defined according to their  $H/D$  value, the ratio of the height of the droplet ( $H$ ) and the diameter of the contacting area between the droplet and the substrate ( $D$ ), as shown in Figure 9. The wettability between the liquid droplets and the steel substrate increases as the  $H/D$  value decreases. Typical droplet shapes and the derived wettabilities from sessile droplet test of  $ZnX_{0.2}$  alloys with ( $X = Ca, Mg, Cu, Ni, Ti, Y, Ce, La, V, Zr$ ) on a 316XV steel substrate under Varigon (95% argon, 5% hydrogen) are listed exemplary in Table 3.

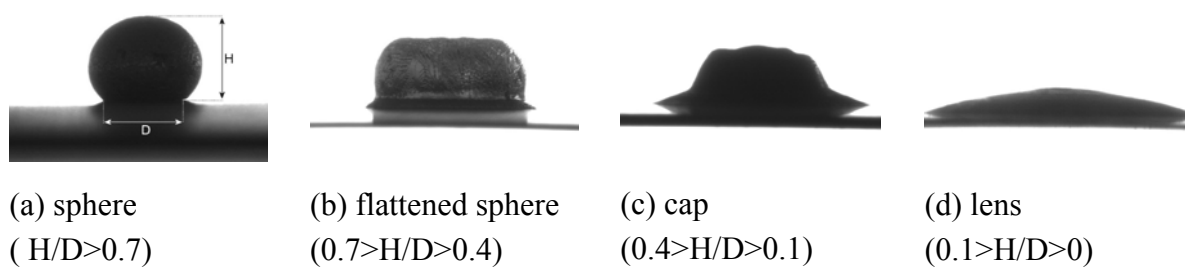


Figure 9: Four types of droplet shapes occurring after contacting of the steel substrate

Obviously the wettability of these  $ZnX_{0.2}$  alloys did not reach the targeted value of a continuous layer and the tendency of the influences of the alloying element is different from that of the finding resulted from the calculation in chapter 2.3. This difference is due to the facts that the wettability of the tested steels is strongly affected by the interaction of the ignoble alloying elements in the Zn alloy as well as in the steel with the atmosphere. Unfortunately the testing device could not fully exclude oxygen access. Since Ca or Mg are well known oxygen affinity elements, they can be easily oxidized and form an oxide film over the droplet surface and then deteriorate the wettability of their Zn alloy, even in atmosphere with very low oxygen partial pressure.

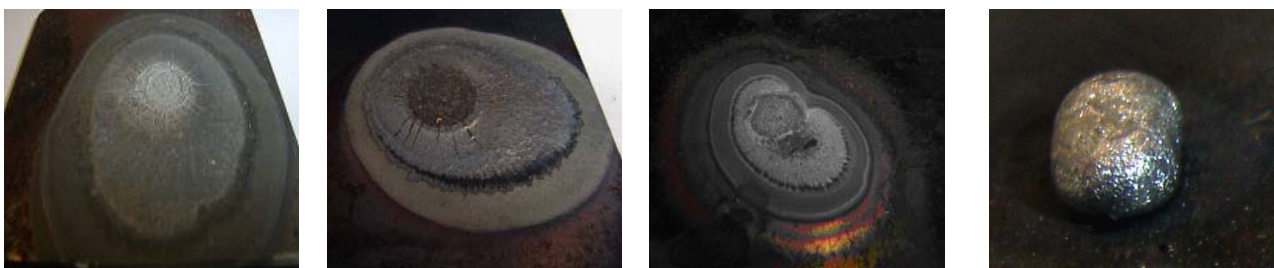


Table 3: Droplet shapes and qualitative wettabilities of ZnX0.2 (X= Ca, Mg, Cu, Ni, Ti, Y, Ce, La, V, Zr) on 31AXV steel substrate under Varigon (95% argon, 5% hydrogen) atmosphere

Droplet shape	sphere	flattened sphere	cap	lens
ZnX alloy ( X=)	Ca, Mg, Cu, Ni, Y	Cu, La, Ni, Y	Ce, La, Ti, V, Zr	Ce, La, V, Zr

“wettability”	very bad	bad	improving	moderate
alloying element	Ca, Mg	Cu, Ni, Y	La, Ti	Ce, V, Zr
calculated effect	Ti, V	Cu, Ni, Zr,	La,Ce,Y	Mg, Ca

By using reductive hydrogen as protecting atmosphere, the adhesion and wettability of the Zn-alloys could be improved a lot compared to Varigon atmosphere, as shown in Figure 10 (c) and (d) exemplary for ZnCe0.2. It can be seen that under Varigon atmosphere, the wettability of a DP500 steel substrate is very bad. When hydrogen is used as protecting atmosphere, the droplet rapidly spreads out flatly when it contacts all three types of steel substrates, as shown in Figure 10 (a) (b) (c). The radius of the coated area reaches about 15 mm at the M3A13 and 31AXV steel substrate, while for the DP500 steel substrate it is smaller. This is certainly caused by surface oxidation of the contained alloying elements (e.g. Mn, Si, Al, Cr, V and Ti) in the DP500 steel, which limit the wettability of the steel surface.



(a) M3A13, H<sub>2</sub>      (b) 31AXV, H<sub>2</sub>      (c) DP500, H<sub>2</sub>      (d) DP500, Varigon

Figure 10: Final form of ZnCe0.2 droplets after contacting different steel substrates under Varigon (95% argon, 5% hydrogen) and pure H<sub>2</sub>

From Figure 10 (a), (b), (c), several diffusion layers can be seen at the final coating, after the liquid ZnCe0.2 alloy droplet spread out over the steel substrate. This may be caused by the interaction diffusion and reaction between Zn and Fe. Direct above the steel substrate, might be a compact layer of intermetallic gamma ( $\Gamma$ ) with a composition of Fe<sub>3</sub>Zn<sub>10</sub> or Fe<sub>5</sub>Zn<sub>21</sub>. The middle layer might



contain the delta ( $\delta$ ) phase layer and zeta ( $\zeta$ ) phase layer. The upper droplet layer solidifying before diffusing away, should be the zinc rich eta ( $\eta$ ) phase layer.

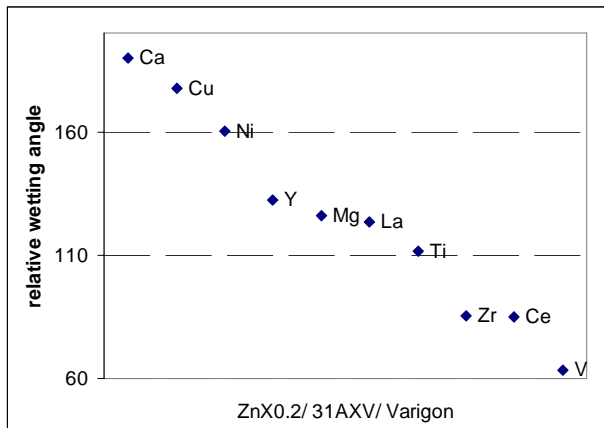
The dynamic change of the shapes of the Zn alloy droplets were recorded by the high speed camera and their wetting angles on steel substrates were measured by the graphical analysis program SCA20. Due to the quick dynamic variation of the droplet shape during the measurements, the pictures of the Zn alloy droplets at the first moment of contacting the steel substrate were taken for comparison. However, as the visibility inside the furnace was low due to the closed installation of the furnace, the comparable low radiation due to moderate temperatures and also due to Zn-evaporation, the sharpness and the contrast of obtained pictures of the droplets were relative low. The analysis program was not able to define the outline and base line of the droplets very exact and it was hardly to obtain an exact value of wetting angles between the droplets and the steel substrates. Therefore, the measured wetting angel values of pure Zn respectively the basis alloy ZnAl0.2 were used as reference values (100%) to compare the measured wetting angles of different ZnX0.05, ZnX0.2, and ZnAl0.2X0.2 alloys, which were obtained at the same conditions as the references. A relative wetting angle value  $\Theta$  of these alloys can be obtained by the following calculation:

$$\Theta = \frac{\theta}{\theta_r} * 100 \quad (13)$$

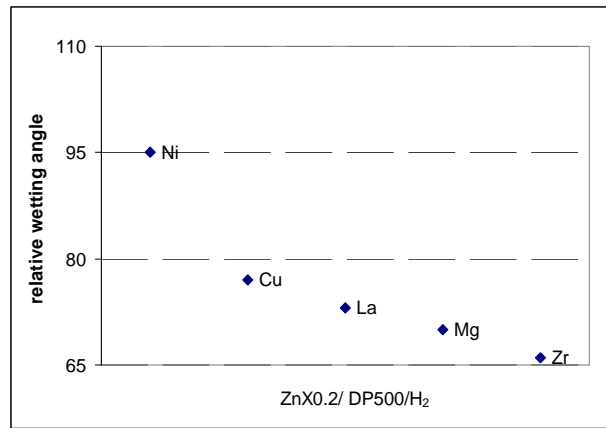
where  $\Theta$  is the relative value of wetting angle;  $\theta$  is the measured value of wetting angle;  $\theta_r$  is the measured value of the wetting angle of reference metals or alloy.

The obtained wetting angles of the investigated alloys obtained at different conditions are summarized in Figure 11. Figure 11 (a) shows the relative values of the wetting angles of the ZnX0.2 alloys on 31AXV low alloyed steel substrates under Varigon (95% argon, 5% hydrogen) atmosphere, using the wetting angle of pure zinc as reference. The corresponding values for DP500 with ZnAl0.2 alloy as reference value are shown in Figure 11 (b), (c), (d), where (b) presents the results of ZnX0.2 alloy, (c) those of ZnX0.05 and (d) those ZnAl0.2X0.2 alloys.

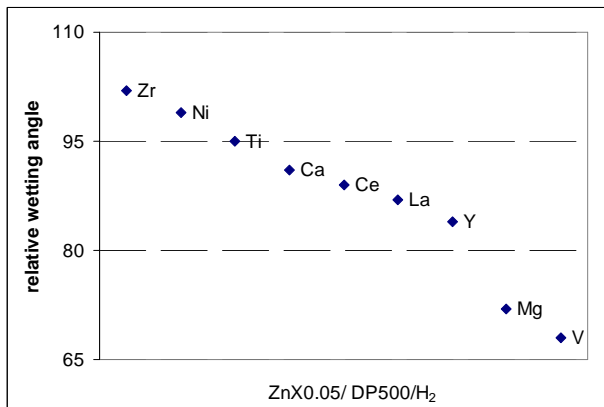
According to their relative value of the wetting angles, the influences of the alloying elements to the wettability of the steel substrate can be classified into three levels: positive, natural and negative influence. Comparing the results of the 0,2% alloyed Zn-/ZnAl-matrix it can be seen, that the un-noble elements Ti, Ce, V, La, Mg, Y and especially Zirconium show a positive effect. This is most probably due to interphase reactions like oxide destruction, which have cleaning effect for the high alloyed steel surface. Despite the careful preconditioning of the steel substrates the remaining oxygen and nitrogen molecules in the flushing gas will be absorbed by the steel alloying elements like Mn and Si forming thin ceramic layers. The presence of very ignoble elements in the Zinc-droplet will lead to cracking of these layers which has a positive influence on the wetting behaviors. In case of the 0.05% alloyed Zn-/ZnAl-matrix this effect is not that significant, most probably due to the fact that the ignoble elements are oxidized and lost by the remaining reactive gas components leading to decreased reduction activities of the Zinc-droplet.



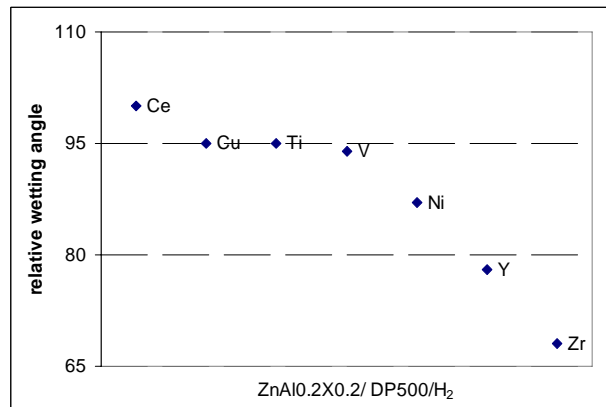
(a)



(b)



(c)



(d)

Figure 11: Relative wetting angles of different ZnX0.05, ZnX0.2, and ZnAl0.2X0.2 alloys: (a) 31AXV steel substrates under Varigon (95% argon, 5% hydrogen) atmosphere; (b) (c) (d) on DP500 steel substrates under pure hydrogen atmosphere

## 4.2 Microscopic analysis of the interface

The ZnV alloy representing a positive influence as well as the ZnCu alloy representing a negative influence on the wettability of Zn, are both here further discussed. The cross sections of the coated DP500 steel substrates were microscopic analyzed under SEM, as shown exemplary in Figure 12. The distribution profiles of the weight percent concentrations of the responding elements over the interface are presented in Figure 13.



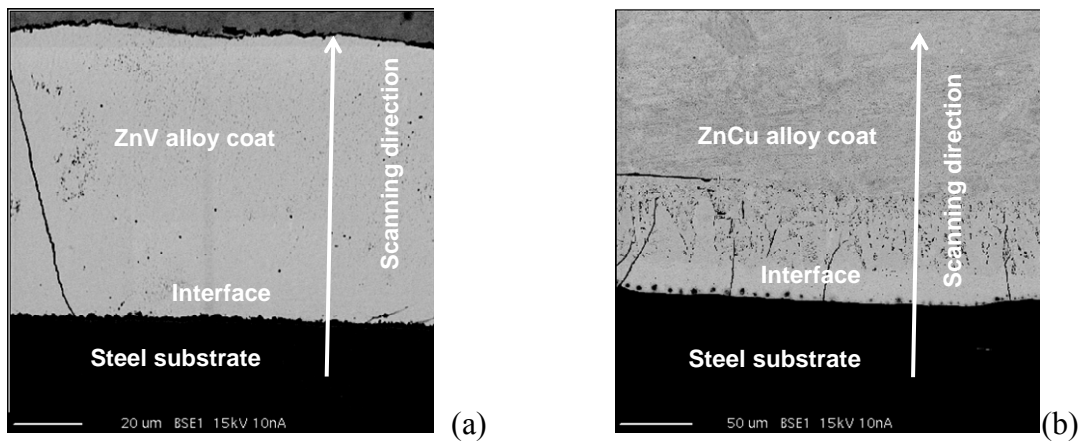


Figure 12: Metallographic cross sections of the coated DP500 steel substrates (a) ZnV alloy (b) ZnCu alloy

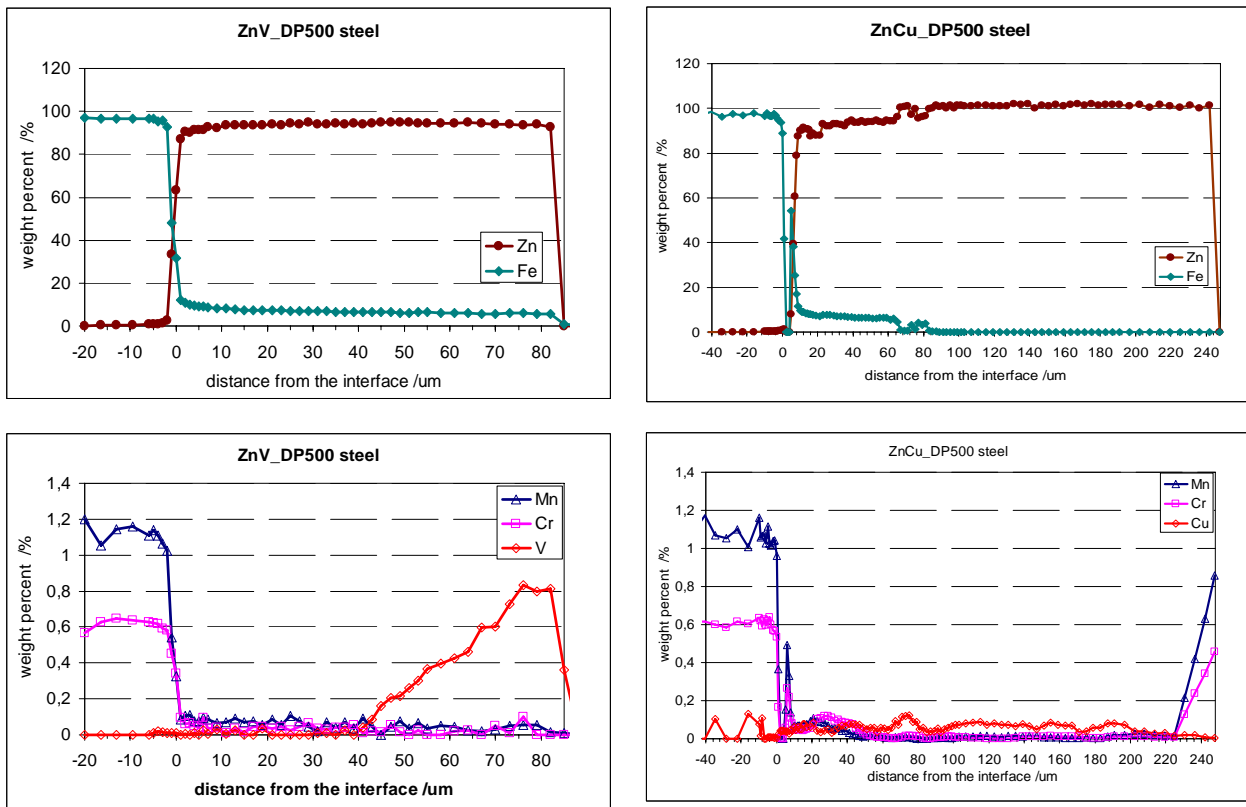


Figure 13: Element concentration profile at the cross section of the ZnV and ZnCu coated DP500 steel substrate

The resulted ZnCu layer (245μm) happens to be much thicker than the ZnV alloy layer (85μm). In both cases the interaction reaction zone between Zn and Fe ranges of about 10μm. The diffusive impregnation depth of Fe into the Zinc-layer is about 85 μm and very large for both alloys. For the ZnV alloy, a high content of the V element is detected close the surface of the droplet, while diffu-





sion of Cr and Mn containing in DP500 steel substrate into the Zn droplet seems to be suppressed. This could be caused by a stronger oxygen affinity of V, which drives this element to diffuse, such inhibiting the oxidation of Cr and Mn. This may be the reason for an improved wettability of the steel substrate. On the other hand for the ZnCu alloy it can be seen that Cu diffuses towards the steel substrate, and due to missing oxygen affine elements a high content of Cr and Mn diffuses towards the surface of the droplet forming an oxide film by gettering the remaining oxygen molecules in the furnace. The next investigations will be focused on the nano-sized interface for further explanation the mechanisms which lead to a better interaction between the solid and the liquid phase.

## 5 Conclusions

The influence of alloying elements, such as Ca, Mg, Cu, Ni, Ti, V, Zr, Y, Ce, La in a Zn bath on the wetting behavior of different types of steel substrates has been investigated. Based on the assumption of ideal solutions, thermochemical modeling has been performed and the surface tensions of many Zinc alloys were calculated. It shows that especially the addition of Ca and Mg decreases the surface tension of the alloy, while V, Ni, Ti, Zr and Cu may increase the surface tension. Nevertheless this view does not include inter phase reactions like oxide destruction, which can have a much stronger influence on wetting.

By using the sessile drop method, the wetting angle between the Zn alloy droplet and the steel substrates were measured. The wetting angles vary dynamically in a very short time after the droplet contacts the steel substrate and a suitable assessment method has been developed. The high alloyed DP500 steel shows a much worse wetting behavior than that of the standard M3A13 and the low alloyed 31AXV steel. Under a reductive hydrogen atmosphere, their wetting behavior can be strongly increased in comparison with that of under a 95% argon/5% hydrogen atmosphere. Among the investigated Zn alloys, V, Zr as an alloying element show the most effective improvement on the wetting behavior with HSS steel sheets.

## 6 Acknowledgement

The financial support from the German Research Foundation (DFG - Deutsche Forschungsgemeinschaft) from 2001-2002 is gratefully acknowledged. The authors would like to thank Dr. Winkler, Dr. Schmitz, Mr. Bünck, and Ms. Jiang for their contributions in this project. Dr. Richter from the institute GFE/ RWTH-Aachen University is also appreciated for carrying out the SEM analysis.



## 7 Reference

- [1] Hot dipping galvanising of high strength steels, steel times International, Dec 2002/ Jan 2003, Vol.27, Issue 1, pp. 9-12.
- [2] Olefjord I., Leijon W., Jelvestam U.: Selective surface oxidation during annealing of steel sheets in H<sub>2</sub>/N<sub>2</sub>, Applied Surface Science, 1980, Vol.6. pp. 241.
- [3] Masahiko, H., Toshio, N., Noriaki, U.: Effect of Si in steel on Hot Dip Galvanizing and Galvannealing, Galvatech' 98, 1998, pp. 221-225.
- [4] Ahrens, M., Bleck, W. and Staudte, J.: Surface condition by reactive gases during continuous annealing of sheet steel, Journal of materials processing Technology, 2001, Vol. 117, pp. 270-275.
- [5] Katiforis, N., Papadimitriou, G.: Influence of Cu, Cd and Sn additions in the galvanizing bath on the structure, thickness and cracking behaviour of the galvanized coating, Surface and Coating Technology, 1996, Vol. 78, pp.185-195.
- [6] Culcasi J.D., Sere P.R., Elsner C.I.: Control of the growth of zinc-iron phases in the hot-dip galvanizing process, Surface and Coating Technology, 1999, Vol. 122, pp. 21-23.
- [7] Lynch R.F.: Hot-Dip Galvanizing Alloys, Journal of Metals, 1987 Aug., pp.39-41.
- [8] Reumont G., Gloriant T., Perrot P.: Experimental influence of the kinetics on galvanized coatings when saturating a zinc bath with alloying elements, Journal of materials science letters, 1996, Vol. 15, pp 445-449.
- [9] Jaycock M.J., Parfitt G.D.: Chemistry of Interfaces, Wiley, NY, 1981, pp. 234.
- [10] Girifalco L.A., Good R.J.: a theory for the estimation of surface and interfacial energies. I. Derivation and application to interfacial tension, Journal of physical chemistry, 1957, Vol.61, pp. 904-909.
- [11] Hajra J. P., Hong-Kee-Lee, Frohberg M.G.: Calculation of the surface tension of liquid binary systems from the data of pure components and the thermodynamic infinite dilution values, Z. Metallkd., 1991, Vol. 82 (8), pp.603-608.
- [12] Hultgren R., Desai P.D., Hawkins D.T., Gleiser M. Kelly K.K.: Selected values of thermodynamic properties of binary alloys, ASM, Metals Park, Ohio, 1973.
- [13] Paradis P-F., Ishikawa T.: Thermophysical properties of molten Yttrium measured by non-contact techniques, Microgravity science technology, 2009, Vol. 21, pp. 113-118.